J. Phase Equilib. Diffus. (2023) 44:714–728
https://doi.org/10.1007/s11669-023-01073-9

ORIGINAL RESEARCH ARTICLE

Phase Equilibria in the Quasi-Ternary System Cu_2Se-In_2Se_3-CuI and the Crystal Structure of the $A^IB^{III}{}_2X^{VI}{}_3Y^{VII}$ Compounds, Where A^I-Cu, Ag; B^{III}-Ga; X^{VI}-Cl, Br, I; Y^{VII}-S, Se, Te

I. A. Ivashchenko[1] · V. S. Kozak[2] · L. D. Gulay[3] · V. V. Galyan[3]

Submitted: 14 March 2023 / in revised form: 20 October 2023 / Accepted: 14 November 2023 / Published online: 6 December 2023

Abstract The quasi-ternary system Cu_2Se-In_2Se_3-CuI has been investigated by x-ray diffraction and differential thermal analysis. The isothermal section at 770 K and the liquidus surface projection of the system have been built. For the first time, the primary crystallization regions, and the coordinates of the invariant and monovariant equilibria have been determined. In the system, the regions of the solid solutions based on the binary, ternary, and quaternary compounds have been investigated. The formation of the $CuIn_2Se_3I$ quaternary compound, which melts congruently at 1213 K and has a homogeneity region of 15 and 9 mol.% CuI within the composition triangle has been established. For the first time, the crystal structures of $CuGa_2Te_3I$ and $AgGa_2Te_3Br$ compounds have been studied using a powder method. They crystallize in the tetragonal symmetry, Space Group I-4, a = 5.9147(4) Å, c = 11.952(2) Å for $CuGa_2Te_3I$; a = 6.2977(3) Å, c = 11.9473(7) Å for $AgGa_2Te_3Br$ compound, respectively. The connection of their structures with the structures of the defective diamond-like semiconductors has been discussed.

Keywords crystal structure · differential thermal analysis · isothermal section · vertical section · x-ray powder diffraction

✉ I. A. Ivashchenko
iivashchenko@pk.edu.pl

[1] Cracow University of Technology, Cracow, Poland

[2] Municipal Institution of Higher Education of the Volyn Oblast Council, Volyn Medical Institute, Lutsk, Ukraine

[3] Lesya Ukrainka Volyn National University, Lutsk, Ukraine

1 Introduction

The multiphase compositions used in semiconductor devices require the study of phase equilibria in multicomponent systems. Therefore, the Cu_2Se-In_2Se_3-CuI system of the mixed 2-anion chalcogen halide type has been chosen for this study. The quasi-ternary system is formed by binary halides and chalcogenides, which already have vast practical application, in particular A^IY^{VII}, where the number of cations is equal to the number of anions (A^I-Cu, Ag; Y^{VII}-Cl, Br, I), cation excess compound $A^I{}_2X^{VI}$, where A^I-Cu, Ag; X^{VI}-S, Se, Te, and cation-defective $B^{III}{}_2X^{VI}{}_3$ compounds, where B^{III}-Ga, In. Since the compounds formed in this system belong to diamond-like semiconductors of the $A^IB^{III}X^{VI}{}_2$ and A^IY^{VII} types, it will be interesting to investigate the interaction between chalcogenides and halides. The construction of the quasi-binary phase diagrams and liquidus surface projection of the quasi-ternary system allows for determining the regions of the primary crystallization of the compounds and the coordinates of the invariant and monovariant equilibria. Previously, we partially investigated the system Cu_2Se-In_2Se_3-CuI and established a character of the $CuIn_2Se_3I$ quaternary compound formation in the In_2Se_3-CuI system.[1] In this work, we present additional results obtained for 3 vertical sections (Cu_3InSe_3-″Cu_3SeI″; ″Cu_3SeI″-$CuIn_2Se_3I$; $CuIn_3Se_5$-$CuIn_2Se_3I$), results for the isothermal section at 770 K and the liquidus surface projection of the quasi-ternary system Cu_2Se-In_2Se_3-CuI. The authors of Ref 2, 3 studied quaternary compounds $A^IB^{III}{}_2X^{VI}{}_3Y^{VII}$, where A^I-Cu, Ag; B^{III}-In; X^{VI}-S, Se, Te; Y^{VII}-Cl, Br, I. Phases with structures of the defective zincblende, spinel, and defective NaCl, respectively, were obtained. For example, it was established that the $CuIn_2Se_3I$ compound crystallizes in the cubic symmetry, Space Group (SG) F-43 m,

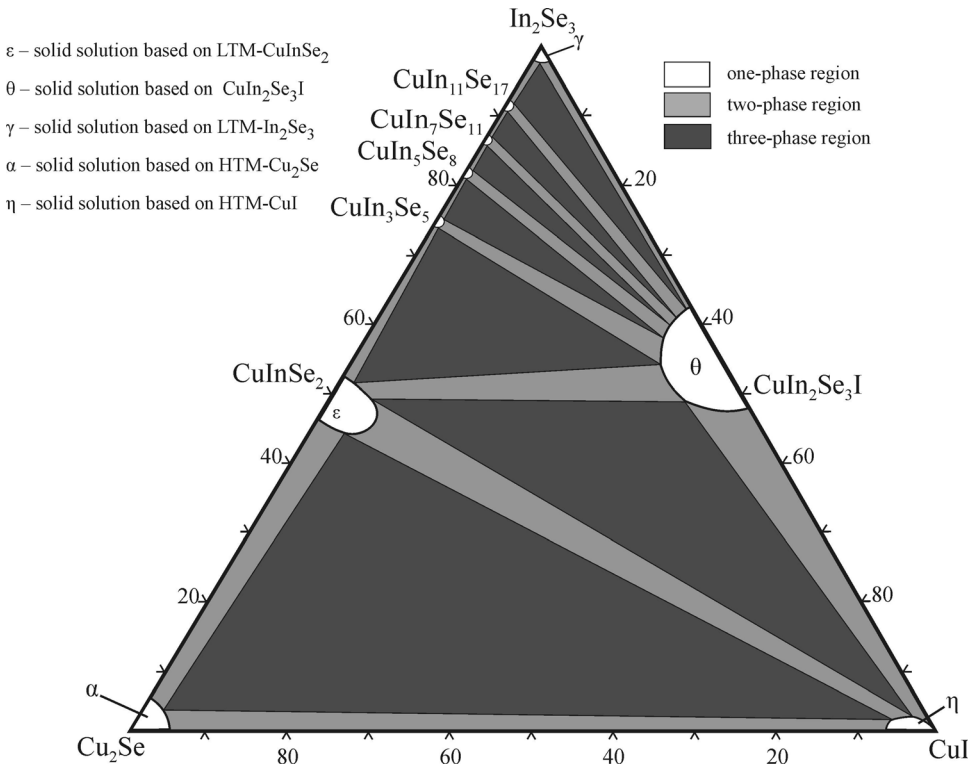

Fig. 1 Isothermal section of the quasi-ternary system Cu_2Se-In_2Se_3-CuI at 770 K

a = 5.781(1) Å.[2] In our work, we decided to investigate the crystal structures of the other quaternary compounds of such type, where B^{III}-Ga. Some of them were investigated by us previously, like $CuGa_2S_3I$,[4] $CuGa_2Se_3I$,[4] $AgGa_2S_3Cl$,[5] $AgGa_2Se_3Cl$,[6] $AgGa_2Se_3Br$,[6] $AgGa_2Te_3Cl$,[7] $AgGa_2Te_3I$.[8] In this work, $CuGa_2Te_3I$ and $AgGa_2Te_3Br$ compounds were synthesized to investigate their crystal structures for a better understanding of the nature of the quaternary compounds. Their crystal structures and connection with known defective semiconductors were discussed.

2 Method of Synthesis

Simple substances of high purity (Cu-99.99, In-99.99, Se-99.997 wt.%) were used to synthesize all alloys of the investigated systems. Cuprous iodide was obtained by the interaction of $CuSO_4 \cdot 5H_2O$ with NaI taken in stoichiometric amounts in the presence of SO_2. During the interaction of the solutions, a brown precipitate was formed, which, after passing SO_2, turned into a white precipitate of cuprous iodide. The precipitate was filtered on a Buchner funnel and washed with water to remove SO_4^{2-} ions. It was washed with ethanol and diethyl ether to prevent the product from oxidizing. The ampoules with prepared weights were evacuated to a residual pressure of $1.33 \cdot 10^{-2}$ Pa and sealed using a gas-oxygen burner. Before the synthesis, pumped and sealed ampoules were placed in metal tubes. The synthesis was carried out in the automatic furnaces ″Thermodent″ with a furnace temperature regulation system of ± 5 K. Samples were synthesized as follows: heating to 670 K at a rate of 10 K/h, annealing for 48 h; heating to a maximum temperature of 1070 K, holding for 48 h; cooling to a temperature of 770 K at a rate of 20 K/h and homogenizing annealing was carried out for 300 h to establish the equilibrium state of the synthesized alloys.[1] They were investigated by x-ray diffraction (XRD) method on DRON 4-13 diffractometer (CuKα radiation) and differential thermal analysis (DTA) (″Thermodent″ H307/1 furnace with a PDA-1 XY-recorder, Pt/Pt-Rh thermocouple). To study the crystal structure of $CuGa_2Te_3I$ and

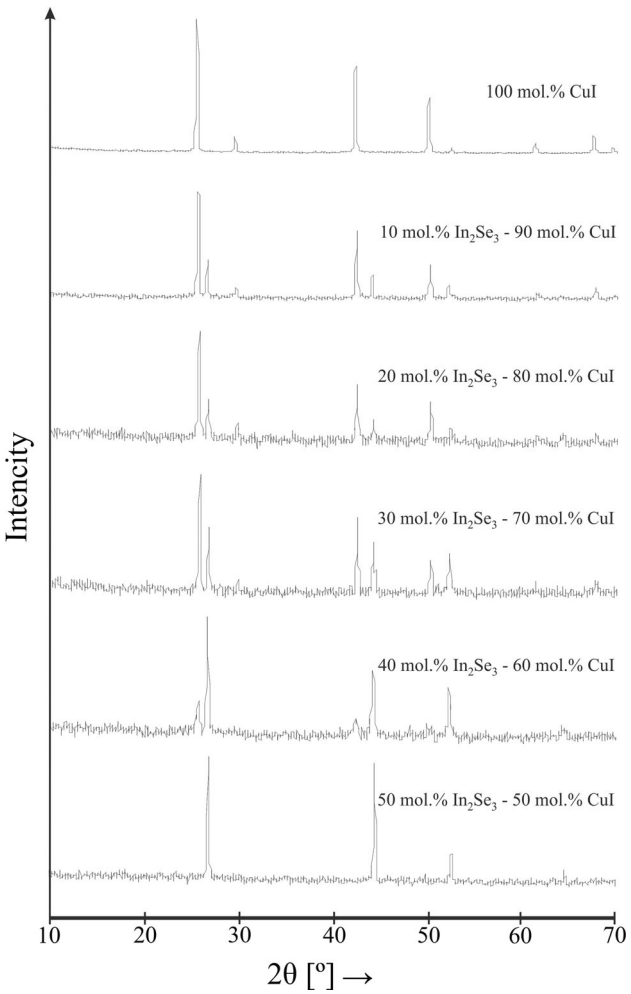

Fig. 2 The diffractograms of the samples of the system In_2Se_3-CuI in the region of 50-100 mol.% CuI

$AgGa_2Te_3Br$, high purity Cu-99.99, Ag-99.99, Ga-99.999 and Te-99.99 wt.% were used. AgBr was obtained by reacting the $AgNO_3$ water solution with the KBr solution.

3 Results and Discussion

3.1 The Isothermal Section of the Quasi-Ternary System Cu_2Se-In_2Se_3-CuI at 770 K (497 °C)

The isothermal section of the quasi-ternary system Cu_2Se-In_2Se_3-CuI at 770 K (497 °C) was constructed based on the results of x-ray diffraction analysis (Fig. 1). According to the obtained data, the CuI compound crystallizes in cubic symmetry, SG $Fm\bar{3}m$, a = 6.1512(3) Å, which agrees well with Ref 9 (Fig. 2). In the system In_2Se_3-CuI, the existence of the quaternary compound $CuIn_2Se_3I$, which crystallizes in cubic symmetry, is confirmed, SG $F\bar{4}3m$, a = 5.8012(1) Å, which is in good agreement with Ref 2. Cu_2Se is indexed as monoclinic symmetry, SG $C2/c$, a = 7.1379 Å, b = 12.3823 Å, c = 27.3904 Å, β = 94.308°.[10] In_2Se_3 is indexed as hexagonal symmetry, SG $P6_3/mmc$, with unit cell periods a = 4.0242(5) Å, c = 19.251(2) Å, which agrees well with Ref 11. The preliminary results of the x-ray phase analysis of the Cu_2Se-In_2Se_3 system were described in our previous work.[12-14] The following ternary compounds were established: $CuInSe_2$, SG $I\bar{4}2d$, a = 5.7855(2) Å, c = 11.551(3) Å; $CuIn_3Se_5$, SG $P\bar{4}2c$, a = 5.7602(1) Å, c = 11.515(3) Å; $CuIn_7Se_{11}$, SG $P3m1$, a = 4.0263(2) Å, c = 16.2992(7) Å; and layered $CuIn_5Se_8$ and $CuIn_{11}Se_{17}$ compounds with unknown structures. The largest single-phase regions in Cu_2Se-In_2Se_3-CuI are based on $CuInSe_2$ and $CuIn_2Se_3I$ compounds. It is known that $CuIn_2Se_3I$ is a cation defect compound, with a ratio of cations to anions of 3:4. In our opinion, this affects the largest extent of the solid solution based on $CuIn_2Se_3I$ towards defective compounds $CuIn_3Se_5$, $CuIn_5Se_8$, $CuIn_7Se_{11}$, $CuIn_{11}Se_{17}$, but not to the $CuInSe_2$ or CuI side, which have the same number of cations and anions. Solubility based on all other binary and ternary compounds is negligible. Between the single-phase regions there are regions of 2-phase equilibria, which divide the system into corresponding 3-phase fields.

3.2 The Liquidus Surface Projection of the Cu_2Se-In_2Se_3-CuI Quasi-Ternary System

The liquidus surface projection (Fig. 3) was built based on the results of the DTA analyses of more than 150 samples (Fig. 4). It consists of fields of primary crystallization of α-solid solution based on HTM-Cu_2Se (e_2-U_1-U_2-p_1-u (e_2-U_1-e_3-Cu_3InSe_3-e_2), ζ-solid solution based on HTM-$CuInSe_2$ (e_3-U_1-U_2-E_1-m_1-E_2-U_3-e_1-U_4-p_4-$CuInSe_2$-e_3), ε-solid solution based on LTM-$CuInSe_2$ (m_1-E_2-p_2-E_1-m_1), η-solid solution based on HTM-CuI (p_1-U_2-E_1-p_2-E_2-U_3-p_3-CuI-p_1), δ-solid solution based on 1-HTM-In_2Se_3 (e_4-E_3-e_5-In_2Se_3-e_4), θ-solid solution based on $CuIn_2Se_3I$ (e_5-E_3-U_5-U_4-e_1-U_3-p_3-$CuIn_2Se_3I$-e_5), compounds $CuIn_5Se_8$ (p_4-U_4-U_5-p_5-p_4),

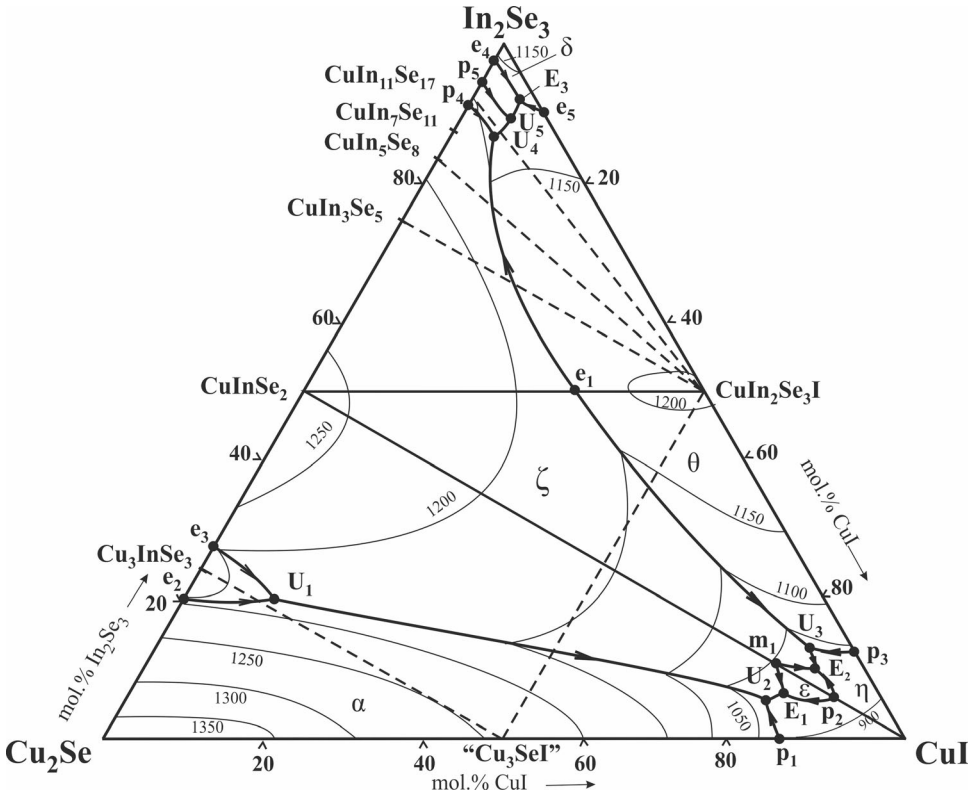

Fig. 3 The liquidus surface projection of the quasi-ternary system Cu_2Se-In_2Se_3-CuI

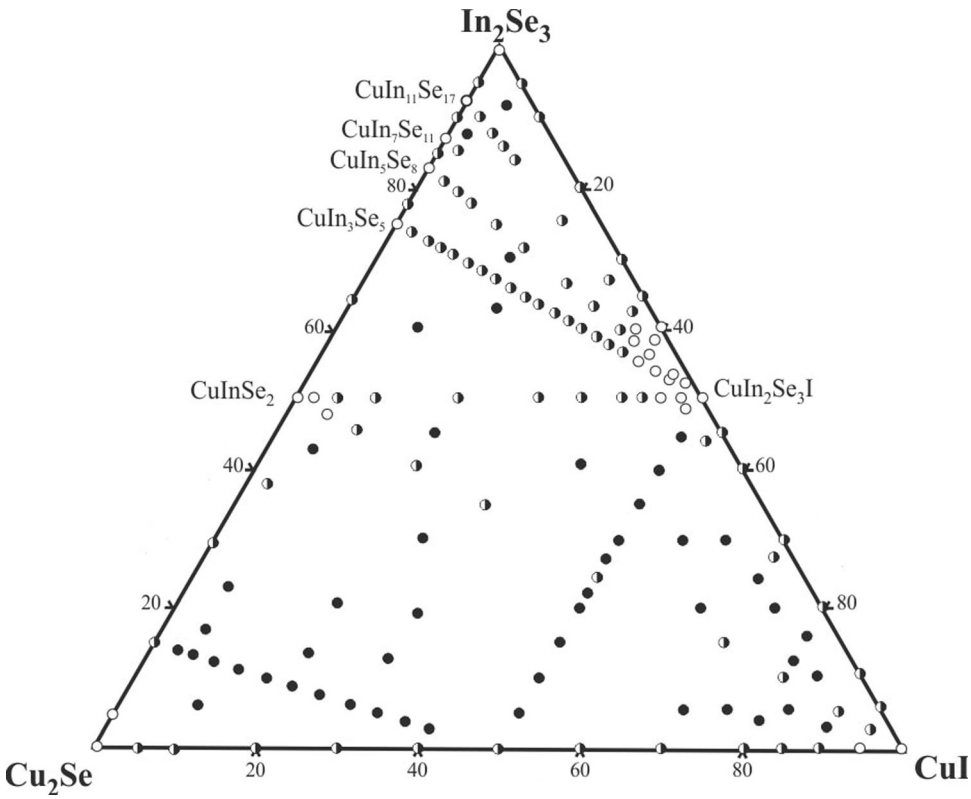

Fig. 4 Phase compositions of the synthesized samples of the quasi-ternary system Cu_2Se-In_2Se_3-CuI

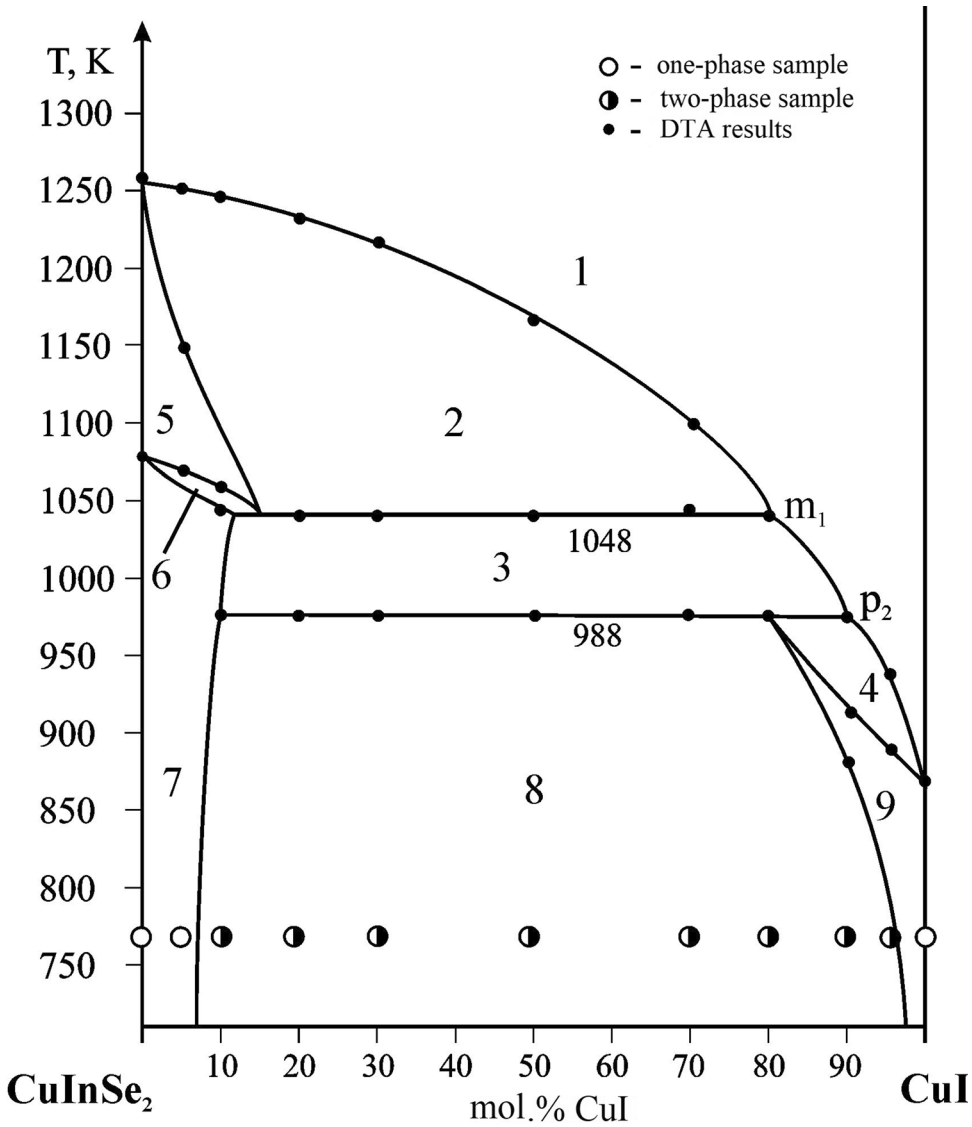

Fig. 5 Phase diagram of $CuInSe_2$-CuI system: 1−L, 2−L + ζ, 3−L + ε, 4−L + η, 5−ζ, 6−ζ + ε, 7−ε, 8-η − ε, 9-η, with ζ and ε-solid solutions based on HTM-$CuInSe_2$ and LTM-$CuInSe_2$, accordingly, η-solid solution based on HTM-CuI[1]

$CuIn_{11}Se_{17}$ (p_5-U_5-E_3-e_4-p_5). These areas are separated by 19 monovariant curves and 19 nonvariant points. The systems $CuInSe_2$-CuI and $CuInSe_2$-$CuIn_2Se_3I$ are quasi-binary (Fig. 5, 6, 7, 8)[1] and divide the investigated quasi-ternary system into 3 subsystems Cu_2Se-$CuInSe_2$-CuI, $CuInSe_2$-$CuIn_2Se_3I$-CuI and $CuInSe_2$-$CuIn_2Se_3I$-In_2Se_3. To simplify the reading of the following text the formulas of the compounds and their polymorphic modifications on which the solid solutions are based will be indicated in parentheses. Three nonvariant transition reactions take place in the first subsystem (Fig. 9). The first one, $L_{U1} + Cu_3InSe_3 \leftrightarrow$ ζ(HTM-$CuInSe_2$) + α(HTM-Cu_2Se), takes place at 1185 K (912 °C). Curves of monovariant processes: $L_{e2\text{-}U1} \leftrightarrow Cu_3InSe_3$ + α(HTM-Cu_2Se), $L_{e3\text{-}U1} \leftrightarrow$ ζ(HTM-$CuInSe_2$) + Cu_3InSe_3 converge to the point U_1. The second nonvariant transition reaction L_{U2} + α(HTM-Cu_2Se) ↔ η(HTM-CuI) + ζ(HTM-$CuInSe_2$) occurs at 1010 K (737 °C). Curves of monovariant processes converge to the point U_2: $L_{U1\text{-}U2} \leftrightarrow$ α(HTM-Cu_2Se) + ζ(HTM-$CuInSe_2$), $L_{p1\text{-}U2} \leftrightarrow$ η(HTM-CuI) + α(HTM-Cu_2Se). Point E_1 lies on

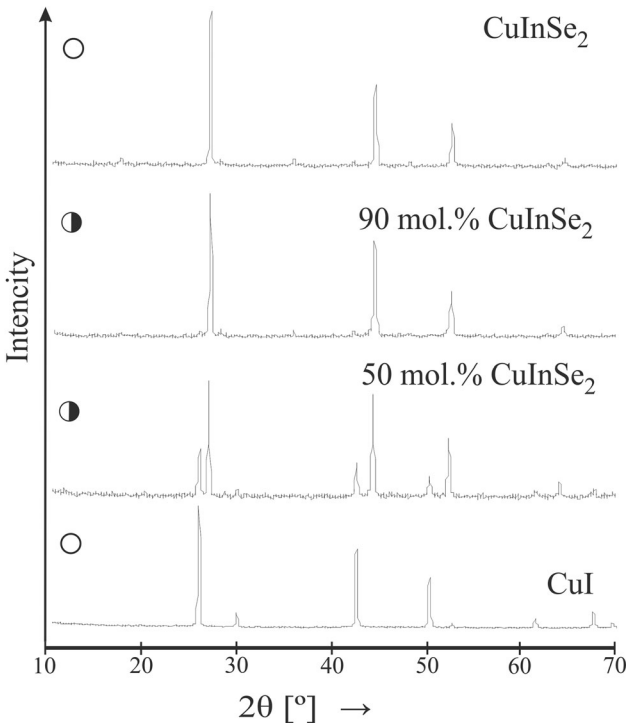

Fig. 6 Some diffractograms of the samples of the $CuInSe_2$-CuI system.

the plane of the nonvariant eutectic process $L_{E1} \leftrightarrow \varepsilon$(LTM-$CuInSe_2$) + η(HTM-CuI) + ζ(HTM-$CuInSe_2$), which takes place at 978 K (705 °C). Curves of monovariant processes converge to this nonvariant point: $L_{U2\text{-}E1} \leftrightarrow$ η(HTM-CuI) + ζ(HTM-$CuInSe_2$), $L_{m1\text{-}E1} \leftrightarrow$ ζ(HTM-$CuInSe_2$)- + ε(LTM-$CuInSe_2$) and $L_{p2\text{-}E1} \leftrightarrow$ η(HTM-CuI) + ε(LTM-$CuInSe_2$). As the temperature decreases, another nonvariant eutectoid process ζ(HTM-$CuInSe_2$) ↔ ε(LTM-$CuInSe_2$) + η(HTM-CuI) + α(HTM-Cu_2Se) occurs in the subsolidus region at 890 K (617 °C). Below it, the alloys contain crystals of 3 phases: ε(LTM-$CuInSe_2$), η(HTM-CuI), α(HTM-Cu_2Se), which agrees with Fig. 1.

In the subsystem $CuInSe_2$-$CuIn_2Se_3I$-CuI the nonvariant process $L_{U3} + \theta(CuIn_2Se_3I) \leftrightarrow$ η(HTM-CuI) + ζ(HTM-$CuInSe_2$) takes place at 1000 K (727 °C). Further, crystallization is completed by the nonvariant eutectic process $L_{E2\text{-}} \leftrightarrow$ η(HTM-CuI) + ε(LTM-$CuInSe_2$) + ζ(HTM-$CuInSe_2$) at 975 K (702 °C), and in the subsolidus region at 900 K (627 °C) the eutectoid process ζ(HTM-$CuInSe_2$) ↔ η(HTM-CuI) + ε(LTM-$CuInSe_2$) + θ($CuIn_2Se_3I$) takes place, and the alloys contain the corresponding 3 phases (Fig. 1). In the subsystem $CuInSe_2$-$CuIn_2Se_3I$-In_2Se_3 the following nonvariant processes take place: $L_{U4} + \zeta(HTM\text{-}CuInSe_2) \leftrightarrow \theta(CuIn_2Se_3\text{-}I) + CuIn_5Se_8$ at 1123 K (850 °C); $L_{U5} + CuIn_5Se_{8\text{-}} \leftrightarrow \theta(CuIn_2Se_3I) + CuIn_{11}Se_{17}$ at 1073 K (800 °C), then crystallization completes through the nonvariant eutectic process $L_{E3} \leftrightarrow \theta(CuIn_2Se_3I) + CuIn_{11}Se_{17} + \delta$(1-HTM-$In_2Se_3$) at 1055 K (782 °C).

Part of the compounds in the system Cu_2Se-In_2Se_3 are formed by solid-phase reactions, namely $CuIn_3Se_5$ and $CuIn_7Se_{11}$. Therefore, there are no regions of the primary crystallization on the liquidus surface projection with them. The Scheil reaction scheme representing the sequence of all invariant reactions is shown on Fig. 9.

3.3 The Vertical Section Cu_3InSe_3-″Cu_3SeI″

The vertical section Cu_3InSe_3-″Cu_3SeI″ was built based on the DTA and x-ray phase analysis results. It passes through 2 surfaces of the primary crystallization of the compound Cu_3InSe_3 and α-solid solution, respectively (Fig. 10). The 3-phase space of secondary crystallization of the binary eutectic $L \leftrightarrow \alpha + Cu_3InSe_3$ descends to the plane of the nonvariant process $L_{U1} + Cu_3InSe_3 \leftrightarrow \alpha + \zeta$, which is shown with a horizontal line at 1185 K (912 °C). There are 3-phase spaces of solid phase decomposition $Cu_3InSe_{3\text{-}} \leftrightarrow \alpha + \zeta$ and monovariant eutectic process $L \leftrightarrow \zeta + \alpha$ below the line at 1185 K (912 °C). The 3-phase space of the eutectic process descends to the plane of the nonvariant process $L_{U2} + \alpha \leftrightarrow \eta + \zeta$ at 1010 K (737 °C), which results in the disappearance of the liquid. At 890 K (617 °C), this section intersects the plane of the eutectoid reaction: ζ(HTM-$CuInSe_2$) ↔ ε(LTM-$CuInSe_2$)- + η(HTM-CuI) + α(HTM-Cu_2Se), below which the alloys are 3-phase ε + η + α in agreement with Fig. 1.

3.4 The Vertical Section ″Cu_3SeI″-$CuIn_2Se_3I$

″Cu_3SeI″-$CuIn_2Se_3I$ was built based on the DTA, x-ray phase analysis results and passes through 2 subsystems Cu_2Se-$CuInSe_2$-CuI and $CuInSe_2$-$CuIn_2Se_3I$-CuI (Fig. 11). The liquidus of the section is represented by the curves of the primary crystallization of α, ζ, θ-solid solutions. In the subsystem Cu_2Se-$CuInSe_2$-CuI, the section crosses the plane of the nonvariant reaction $L_{U2} + \alpha \leftrightarrow \eta + \zeta$ at 1010 K (737 °C), resulting in one region where the liquid disappears for some of the compositions (field 14, the

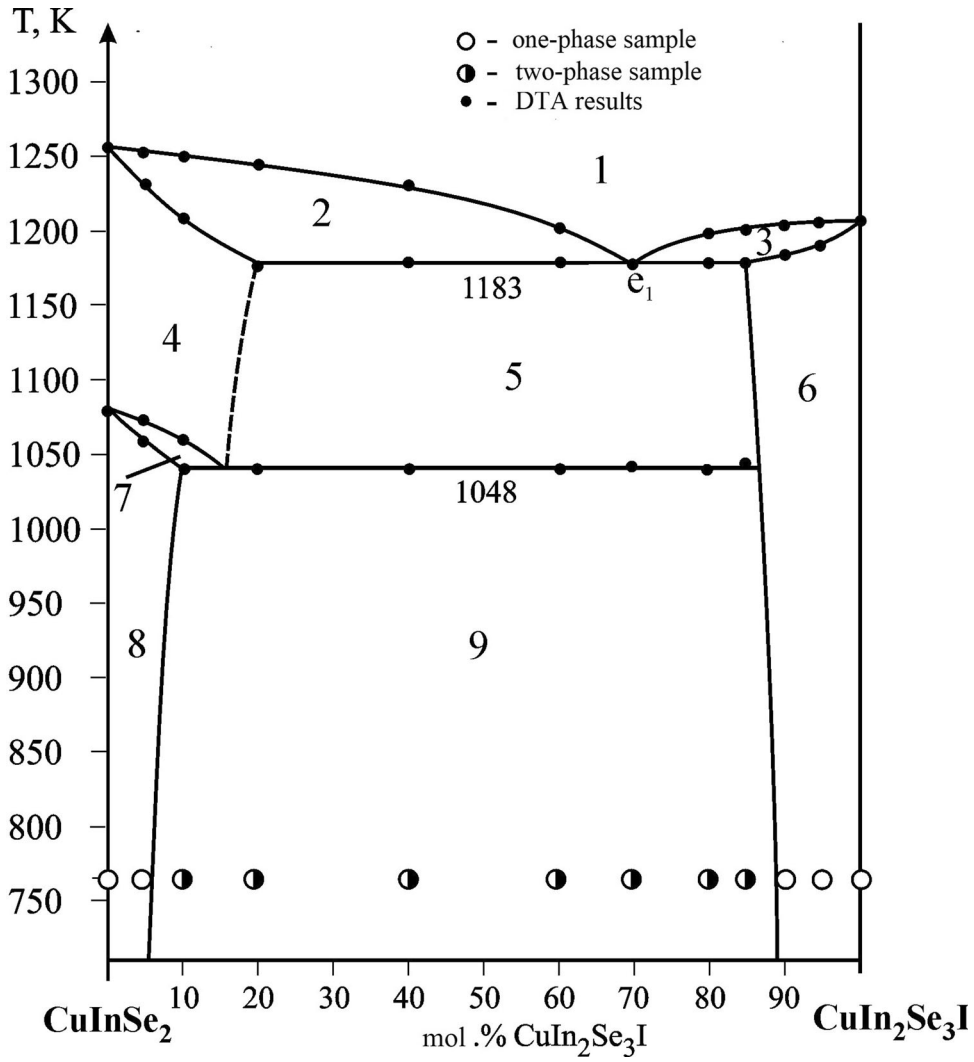

Fig. 7 Phase diagram of $CuInSe_2$-$CuIn_2Se_3I$ system: 1−L, 2−L + ζ, 3−L + θ, 4−ζ, 5−ζ + θ, 6−θ, 7−ζ + ε, 8−ε, 9−ε + θ, with ζ-solid solution based on HTM-$CuInSe_2$, ε-solid solution based on LTM-$CuInSe_2$, θ-solid solution based on $CuIn_2Se_3I$[1]

3-phase (α + η + ζ) region) while in the other region the crystals of α-solid solution disappear. Therefore, below the horizontal at 1010 K (737 °C) is field 12, where the monovariant eutectic process L ↔ η + ζ occurs. This field, together with the 3-phase field 10 (L + ε + η) of the monovariant eutectic process L ↔ ε + η, descends to the plane of nonvariant eutectic process L_{E1} ↔ ε + η + ζ at 978 K (705 °C). At 890 K (617 °C), this section intersects the plane of the nonvariant eutectoid reaction ζ(HTM-$CuInSe_2$) ↔ ε(LTM-$CuInSe_2$) + η(HTM-CuI) + α(HTM-Cu_2Se). Below this plane, the alloys are 3-phase and contain crystals of ε, η, α -solid solutions (field 17), which agrees with the isothermal section in Fig. 1.

In the subsystem $CuInSe_2$-$CuIn_2Se_3I$-CuI at 1000 K (727 °C), the section intersects the plane of the nonvariant process L_{U3} + θ ↔ η + ζ, which results in the disappearance of the liquid only in a part of the alloys of the section, that is why field 7 contains 3 phases: θ + η + ζ. In the other part of the section, the nonvariant transition reaction L_{U3} + θ ↔ η + ζ results in the disappearance of the θ-solid solution. Therefore, below the horizontal at 1000 K (727 °C) is field 9, where the monovariant eutectic process L ↔ η + ζ takes place, which together with the 3-phase field L + ε + η of the monovariant eutectic process L ↔ ε + η descends to the plane of the nonvariant eutectic process L η + ε + ζ at 975 K (702 °C). The vertical section

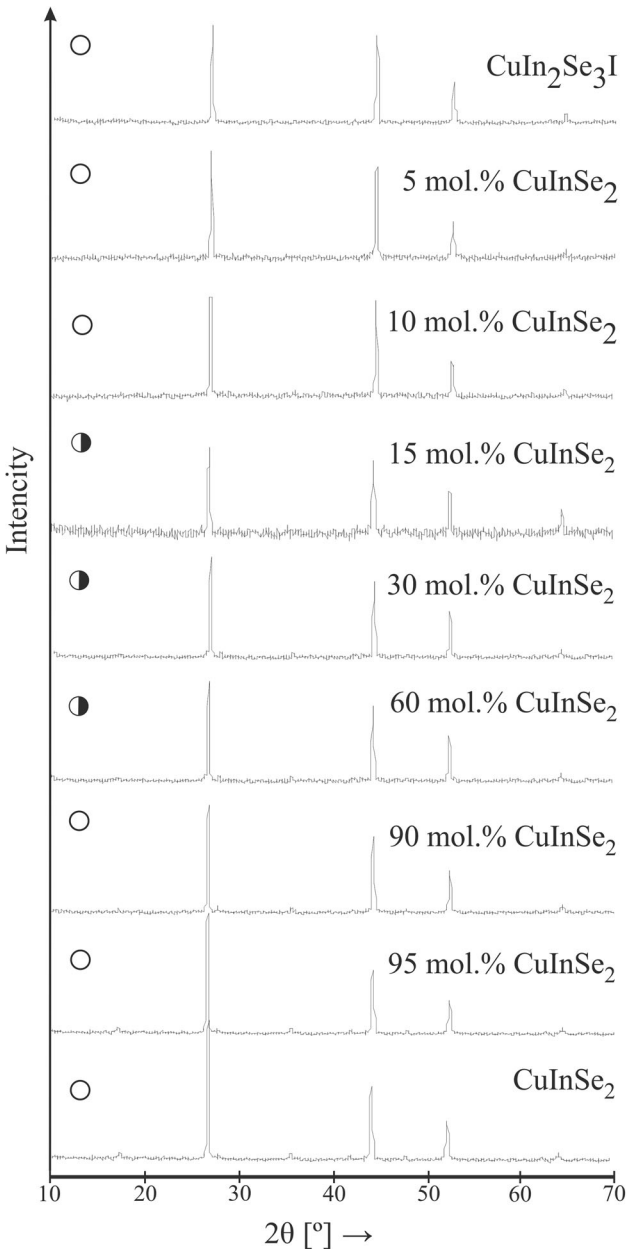

Fig. 8 Some diffractograms of the samples of the $CuInSe_2$-$CuIn_2Se_3I$ system

intersects the plane of the nonvariant eutectoid decomposition $\zeta(\text{HTM-CuInSe}_2) \leftrightarrow \eta(\text{HTM-CuI}) + \varepsilon(\text{LTM-CuInSe}_2) + \theta(\text{CuIn}_2\text{Se}_3\text{I})$ at 900 K (627 °C). Below this plane, the alloys are 3-phase and contain the crystals of η, ε, θ-solid solutions (field 20), which agrees with Fig. 1. The region between fields 7 and 8, is 2-phase η + ζ, since the process $L_{U3} + \theta \leftrightarrow \eta + \zeta$ at 1000 K (727 °C) for the composition of 30 mol.% ″Cu_3SeI″-70 mol.% $CuIn_2Se_3I$ ends with the disappearance of the liquid and the crystals of θ-solid solution because this composition coincides with the connecting horizontal of the plane of the nonvariant process $L_{U3} + \theta \leftrightarrow \eta + \zeta$.

3.5 The Vertical Section $CuIn_3Se_5$-$CuIn_2Se_3I$

The section was built based on the DTA results and x-ray phase analysis. The the regions with liquid (Fig. 12) are represented by the areas of primary crystallization of ζ-solid solution based on HTM-$CuInSe_2$ and θ-solid solution based on $CuIn_2Se_3I$. The section intersects the plane of the nonvariant process $L_{U4} + \zeta \leftrightarrow \theta + CuIn_5Se_8$ at 1123 K (850 °C) where for compositions in this section the liquid disappears. In the subsolidus region, 2 planes of nonvariant processes $\zeta \leftrightarrow \theta + CuIn_5Se_8 + Cu_2In_4Se_7$ (1080 K) (807 °C), $CuIn_5Se_8 + Cu_2In_4Se_7 \leftrightarrow \xi + \theta$ (1030 K) (757 °C) intersect with the section, where ξ is solid solution based on $CuIn_3Se_5$. In alloys of this section, this results in the disappearance of $CuIn_5Se_8$ and $Cu_2In_4Se_7$ crystals, so below 1030 K (757 °C), crystals of ξ- and θ-solid solutions are present which agrees with Fig. 1. As the temperature decreases to 770 K (497 °C), the limit of ξ - solid solution decreases to 3 mol.% of the second component. The parameters of the unit cell increase a little from a = 5.7602(1) Å, c = 11.515(3) Å for $CuIn_3Se_5$ till a = 5.7657(2) Å, c = 11.525(4) Å for the composition of 95 mol.% $CuIn_3Se_5$-5 mol.% $CuIn_2Se_3I$. The region of θ-solid solution narrows to 17 mol.% $CuIn_3Se_5$ with a decrease in temperature to 770 K (497 °C). The parameter of the unit cell decreases from a = 5.8012(1) Å for $CuIn_2Se_3I$ till a = 5.7722(3) Å for the composition of 20 mol.% $CuIn_3Se_5$-80 mol.% $CuIn_2Se_3I$.

3.6 Crystal Structure of $A^IB^{III}{}_2X^{VI}{}_3Y^{VII}$ Compounds, Where A^I-Cu, Ag; B^{III}-Ga; X^{VI}-Cl, Br, I; Y^{VII}-S, Se, Te

When the In_2Se_3-CuI system was investigated in Ref 1, the formation of the quaternary compound $CuIn_2Se_3I$, which belongs to a larger group of compounds with general formula $A^IB^{III}{}_2X_3Y$ (A^I-Cu, Ag; B^{III}-Ga, In; X-S, Se, Te; Y-Cl, Br, I) was established. Replacing Cu^+, In^{3+}, Se^{2-} and I^- by Ag^+, Ga^{3+}, Te^{2-}, and Br^- the quaternary

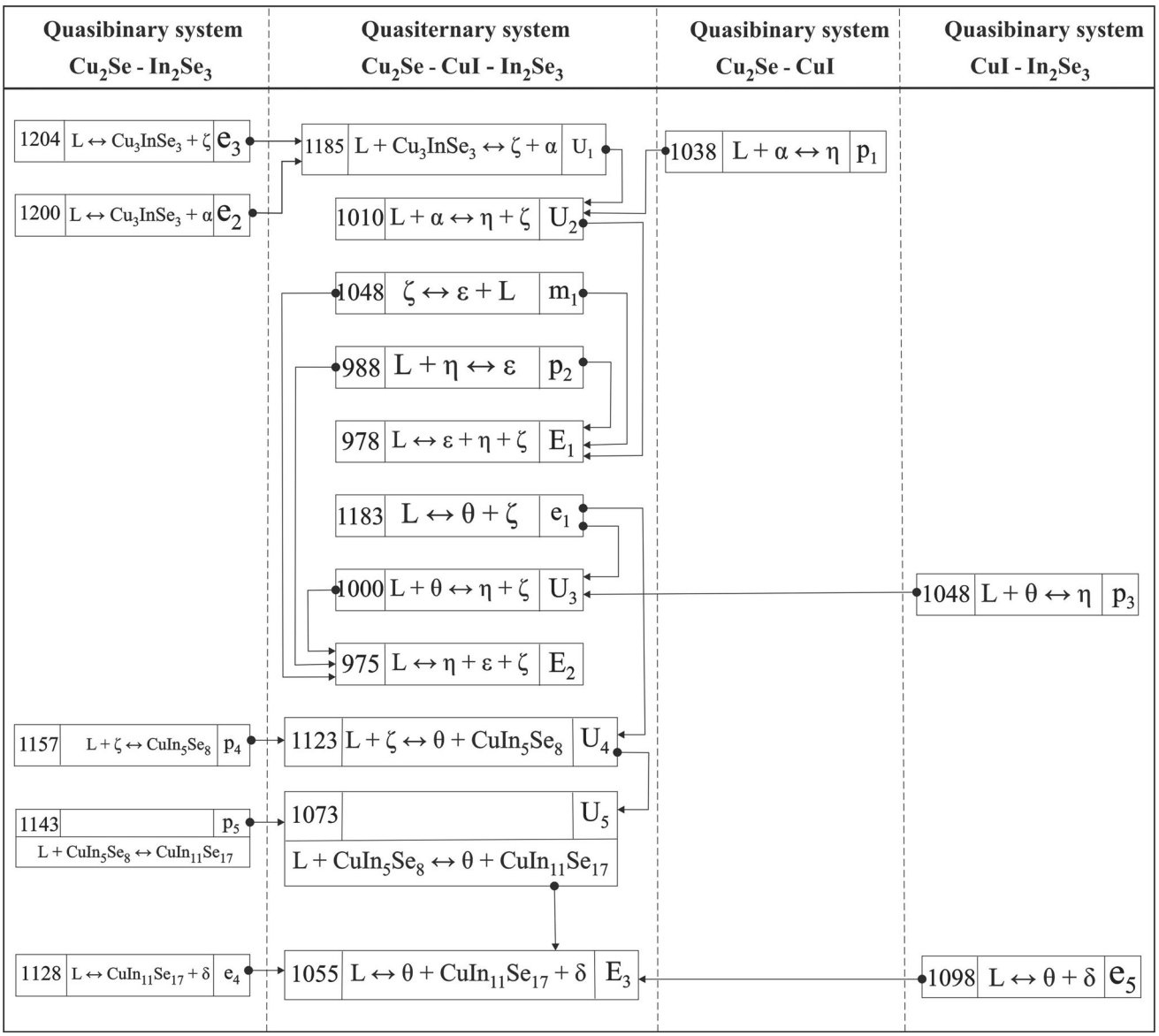

Fig. 9 Scheil reaction scheme of the quasi-ternary system Cu_2Se-In_2Se_3-CuI

compounds $CuGa_2Te_3I$, $AgGa_2Te_3Br$ are obtained, for which the crystal structures were studied using the powder method. The measurement conditions and the calculation results are shown in Tables 1, 2, 3, 4, Fig. 13, 14. The coordinates and the isotropic thermal parameters of atoms in the structures of the $CuGa_2Te_3I$ and $AgGa_2Te_3Br$ are given in Tables 2 and 3. The interatomic distances and coordination numbers of the atoms are shown in Table 4. The Ga atoms occupy 2 Wyckoff positions 2*a* and 2*c*, have tetrahedral coordination and occupy these positions to 80% (Tables 2, 3; Fig. 15). 2 Wyckoff positions (2*b,* 2*d*) are occupied by the statistical mixtures M1 (Cu (Ag) + Ga) and M2 (Cu (Ag) + Ga), resulting in coordination polyhedron-tetrahedron [M1 4Te], [M2 4Te]. The statistical mixtures M1 and M2 are 50% Cu (Ag) and 20% Ga, and 30% of positions are not occupied.

As previously mentioned, chalcohalides of the type $A^{I}C^{III}{}_2X^{VI}{}_3Y^{VII}$ belong to cation-deficient compounds with a

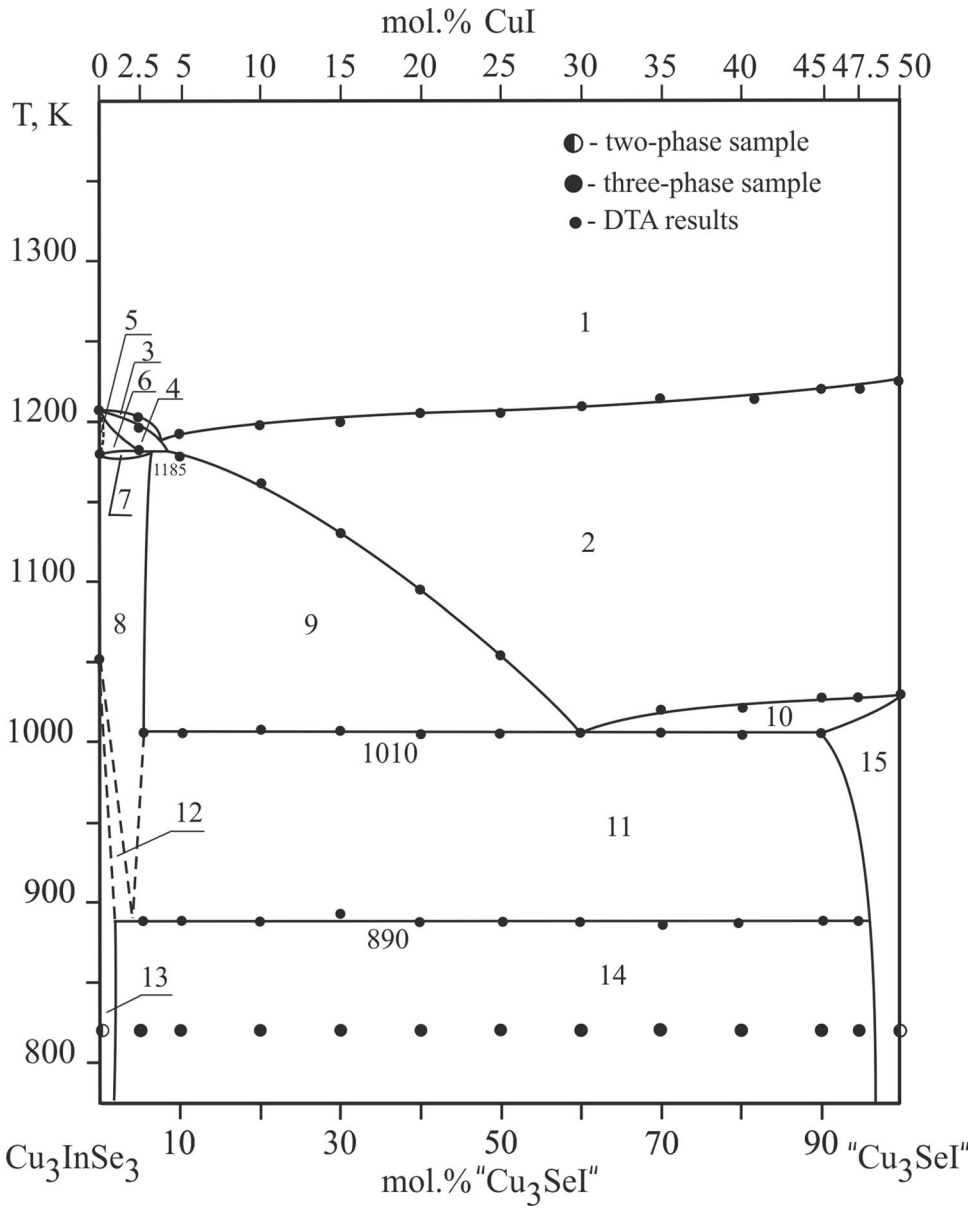

Fig. 10 The vertical section Cu_3InSe_3-"Cu_3SeI": 1−L; 2−L + α; 3−L + Cu_3InSe_3; 4−L + α + Cu_3InSe_3; 5−Cu_3InSe_3; 6−Cu_3InSe_3 + α; 7−Cu_3InSe_3 + α + ζ; 8−α + ζ; 9−L + α + ζ; 10−L + α + η; 11−L + η + ζ; 12−α + ζ + ε; 13−α + ε; 14−α + η + ε; 15−η + α, with ζ-solid solution based on HTM-$CuInSe_2$, ε-solid solution based on LTM-$CuInSe_2$, α-solid solution based on Cu_2Se, η-solid solution based on CuI

ratio of cations to anions of 3:4. The structure can be represented as a 3-layer packing of anions in which ¾ of the tetrahedral vacancies are occupied by C^{III} cations, for example, Ga or In. Statistical mixtures of M1 (Cu(Ag) + Ga) and M2 (Cu(Ag) + Ga), and ¼ of the voids remain vacant.[15] According to Ref 16, other compounds have a cation:anion ratio of 3:4, for example, $AgIn_5Se_8$, $AgZnPS_4$, Cu_2HgI_4, and Hg_2SnSe_4. A similar ratio have $CdGa_2Se_4$ and β-Ag_2HgI_4, structural type $CdAl_2S_4$, both crystallize in the SG *I*-4. In the specified structures of the studied compounds $A^IC^{III}{}_2X^{VI}{}_3Y^{VII}$ and $CdGa_2Se_4$, β-Ag_2HgI_4, a similar arrangement of cations is observed (Table 5), but in $A^IC^{III}{}_2X^{VI}{}_3Y^{VII}$ the A^I atoms half occupy 2 positions 2*b*, 2*d*. The C^{III} cations are statistically in the same positions as A^I, filling them to 20%. The C^{III} positions, 2*a* and 2*c*, remain partially occupied at 80%. In the compounds $CdGa_2Se_4$ and β-Ag_2HgI_4, position 2*a* is occupied by a divalent cation, and position 2*c* and 2*b*-by other cations in the structure (Ga and Ag, respectively). The vacancy occupies the 2*d* position in these structures.

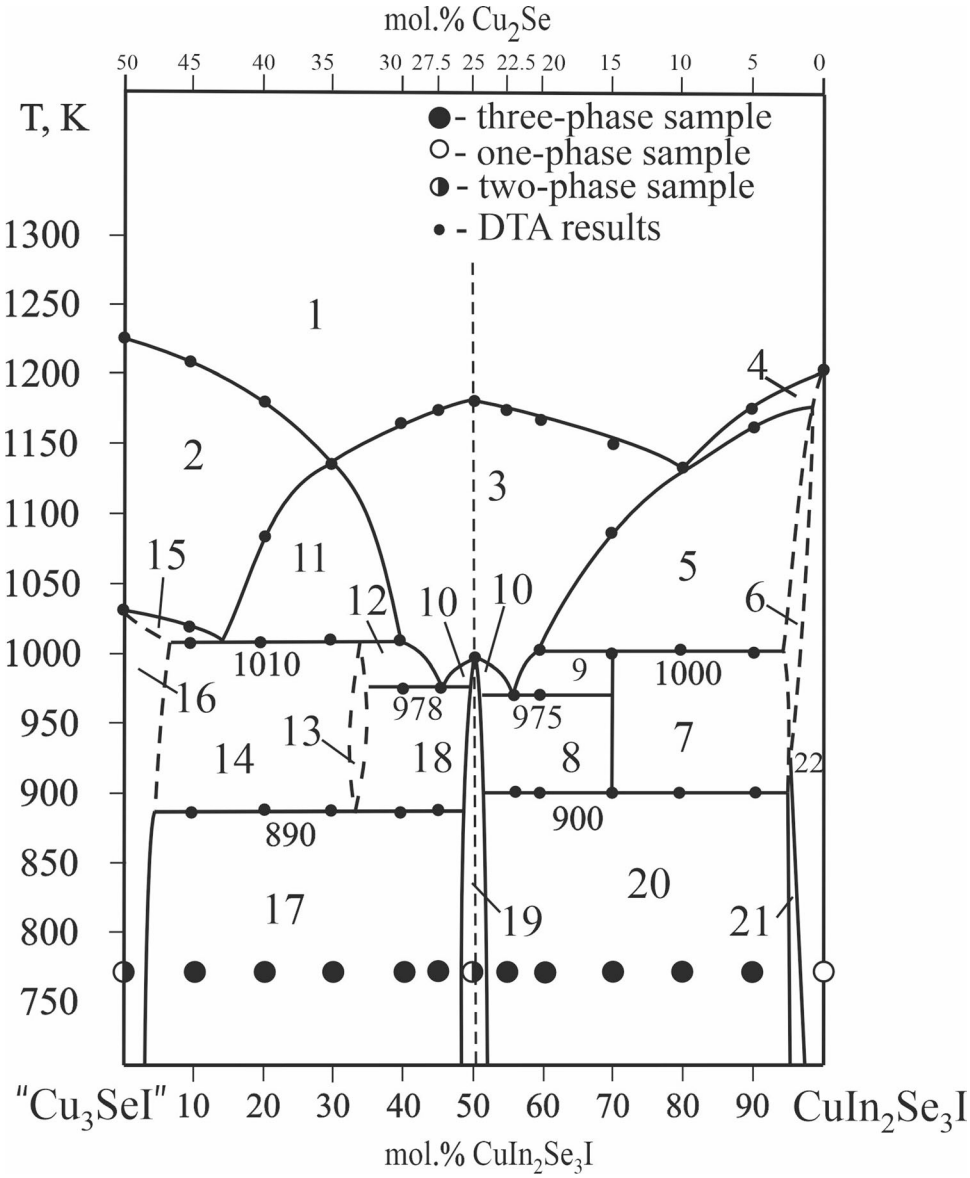

Fig. 11 The vertical section "Cu_3SeI"-$CuIn_2Se_3I$: 1−L; 2−L + α; 3−L + ζ; 4−L + θ; 5−L + θ + ζ; 6−θ + ζ; 7−ζ + η + θ; 8−η + ε + ζ; 9−L + ζ + η; 10−L + ε + η; 11−L + ζ + α; 12−L + ζ + η; 13−ζ + η; 14−α + ζ + η; 15−L + α + η; 16−α + η; 17−α + ε + η; 18−ζ + ε + η; 19−η + ε; 20−η + ε + θ; 21−η + θ; 22−θ, with ζ-solid solution based on HTM-$CuInSe_2$, ε-solid solution based on LTM-$CuInSe_2$, θ-solid solution based on $CuIn_2Se_3I$, α-solid solution is based on Cu_2Se, η-solid solution based on CuI.

The composition of the cation-deficient compounds with a ratio of cations to anions of 3:4 can be represented by the formula $K_{n-u}\square_uA_n$, where K-cations, □-vacancies, A-anions, and u-the first letter of the word "unoccupied", which indicates the number of vacancies. For these compounds $VEC > 4$, in particular, $AgIn_5Se_8$, $AgZnPS_4$, Cu_2HgI_4, and Hg_2SnSe_4, VEC = 4.571.[17, 18] The exact value is obtained for the quaternary chalcohalides $A^IC^{III}{}_2X^{VI}{}_3Y^{VII}$ (1·1 + 2·3 + 3·6 + 1·7)/1 + 2 + 3 + 1 = 4.571. If we consider the vacancy as an atom with zero valence, then we get for the compounds $A^IC^{III}{}_2\square X^{VI}{}_3Y^{VII}$ 1·1 + 2·3 + 1 0 + 3·6 + 1·7)/1 + 2 + 1 + 3 + 1 = 4, which means that their structures are tetrahedral when the cations are surrounded by the 4 nearest anions located at the vertices of the tetrahedron.

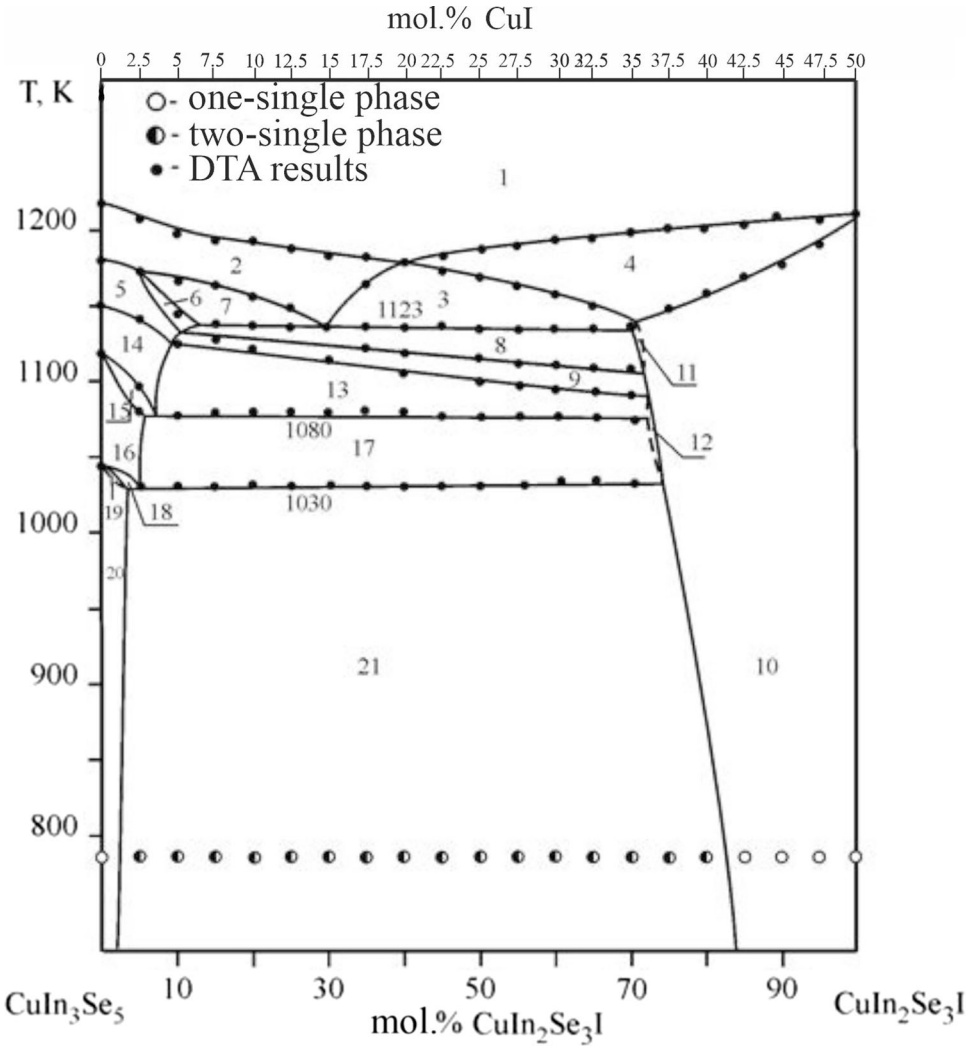

Fig. 12 The vertical section $CuIn_3Se_5$-$CuIn_2Se_3I$: 1−L, 2−L + ζ, 3−L + ζ + θ, 4−L + θ, 5−ζ, 6−$CuIn_5Se_8$ + ζ, 7−L + $CuIn_5Se_8$ + ζ, 8−θ + $CuIn_5Se_8$ + ζ, 9−ζ + θ, 10−θ, 11−ζ + θ, 12−$Cu_2In_4Se_7$ + θ, 13−$Cu_2In_4Se_7$ + ζ + θ, 14−$Cu_2In_4Se_7$ + ζ, 15−$Cu_2In_4Se_7$ + $CuIn_5Se_8$ + ζ, 16−$CuIn_5Se_8$ + $Cu_2In_4Se_7$, 17−$CuIn_5Se_8$ + $Cu_2In_4Se_7$ + θ, 18−$Cu_2In_4Se_7$ + $CuIn_5Se_8$ + $CuIn_3Se_5$, 19−$Cu_2In_4Se_7$ + $CuIn_3Se_5$, 20−$CuIn_3Se_5$ (ξ), 21−$CuIn_3Se_5$ + θ, with ζ-solid solution based on HTM-$CuInSe_2$, θ-solid solution based on $CuIn_2Se_3I$

4 Conclusions and Future Work

The quasi-ternary system Cu_2Se-In_2Se_3-CuI formed by binary halides and chalcogenides, which already have wide practical applications, has been investigated by x-ray and differential thermal methods. The isothermal section at 770 K (497 °C) and the liquidus surface projection of the system have been built. The regions of primary crystallization, types, and coordinates of the invariant and monovariant equilibria have been established for the first time. It allows us to know the areas of primary crystallization of the compounds, types and the coordinates of the invariant and monovariant equilibria. In the system, the regions of the solid solutions based on the binary, ternary,

and quaternary compounds have been investigated. The formation of the $CuIn_2Se_3I$ quaternary compound, which melts congruently at 1213 K (940 °C) and has a homogeneity region of 15 and 9 mol.% CuI in the composition triangle, has been established. For the first time, the crystal structures of $CuGa_2ITe_3$ and $AgGa_2BrTe_3$ compounds, which belong to the cation-deficient compounds $A^IC^{III}{}_2X^{VI}{}_3Y^{VII}$ with a ratio of cations to anions of 3:4, have been studied using a powder method. They crystallize in the tetragonal symmetry, SG *I*-4, a = 5.9147(4) Å, c = 11.952(2) Å for $CuGa_2ITe_3$; a = 6.2977(3) Å, c = 11.9473(7) Å for $AgGa_2BrTe_3$ compound. The connection of their structures with the structures of the defect diamond-like semiconductors has been discussed, and a conclusion about their semiconducting properties has been made.

According to the results, future work will be on growing the single crystals of the quaternary compound $CuIn_2Se_3I$ and solid solutions formed in the system to investigate their semiconducting properties.

Table 1 Results of crystal structure refinement of the $CuGa_2Te_3I$, $AgGa_2Te_3Br$ compounds

Empirical formula	$CuGa_2Te_3I$	$AgGa_2Te_3Br$
Sp. Gr	*I*-4	*I*-4
Z	2	2
Unit cell parameters, Å	a = 5.9147(4), c = 11.952(2)	a = 6.2977(3), c = 11.9473(7)
V, Å^3	418.1(1)	473.85(7)
Number of atoms in cell	14	14
Calculated density, g/cm^3	5.660(2)	4.9759(7)
Absorption coefficient, 1/cm	1255.51	1043.46
Radiation and wavelenght, Å	CuKα; 1.54185	CuKα; 1.54185
Diffractometer	DRON 4-13	DRON 4-13
Mode of refinement	Full profile	Full profile
Number of free parameters	10	10
R_I; R_p	0.0902; 0.3759	0.1031; 0.2576
Scale factor	1.26(3)	1.96(10)
Texture axis and parameter	[1 0 0] 0.37(3)	[0 1 1] 0.14(3)

Table 4 Interatomic distances and coordination numbers, C.N. of atoms in the $CuGa_2Te_3I$, $AgGa_2Te_3Br$ structures

$CuGa_2Te_3I$		$AgGa_2Te_3Br$	
Atoms	Interatomic distances, Å		C.N.
Ga1-4An	2.55(4)	2.69(2)	4
Ga2-4An	2.58(4)	2.60(2)	4
M1-4An	2.61(4)	2.69(2)	4
M2-4An	2.54(4)	2.751(15)	4

Table 2 Refined coordinates of atoms and their isotropic thermal parameters in $CuGa_2Te_3I$

Atom	Wyck off positions	*x/a*	*y/b*	*z/c*	Occupation	$B_{isot.} \times 10^2$, Å^2
Ga1	2*a*	0	0	0	0.8	0.75(11)
Ga2	2*c*	0	½	¼	0.8	0.74(11)
M1	2*b*	0	0	½	0.5 Cu + 0.2 Ga	0.76(11)
M2	2*d*	0	½	¾	0.5 Cu + 0.2 Ga	0.76(11)
An	8 *g*	0.248(7)	0.243(9)	0.127(3)	0.75 Te + 0.25 I	0.18(7)

Table 3 Refined coordinates of atoms and their isotropic thermal parameters in $AgGa_2Te_3Br$

Atom	Wyck off positions	*x/a*	*y/b*	*z/c*	Occupation	$B_{izot.} \times 10^2$ Å^2
Ga1	2*a*	0	0	0	0.8	0.54(6)
Ga2	2*c*	0	½	¼	0.8	0.54(6)
M1	2*b*	0	0	½	0.5 Ag + 0.2 Ga	0.35(6)
M2	2*d*	0	½	¾	0.5 Ag + 0.2 Ga	0.34(6)
An	8 *g*	0.2402(12)	0.2602(11)	0.126(2)	0.75 Te + 0.25 Br	0.44(4)

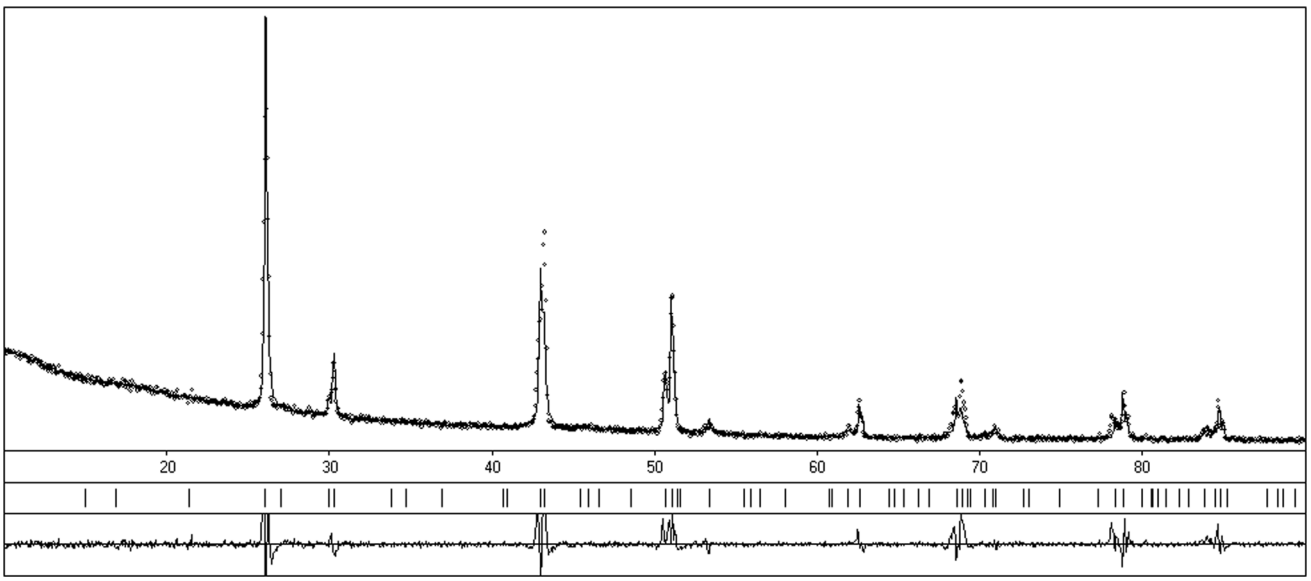

Fig. 13 Experimental (dots), calculated (solid) and difference (bottom scale) diffractogram of the $CuGa_2Te_3I$ compound

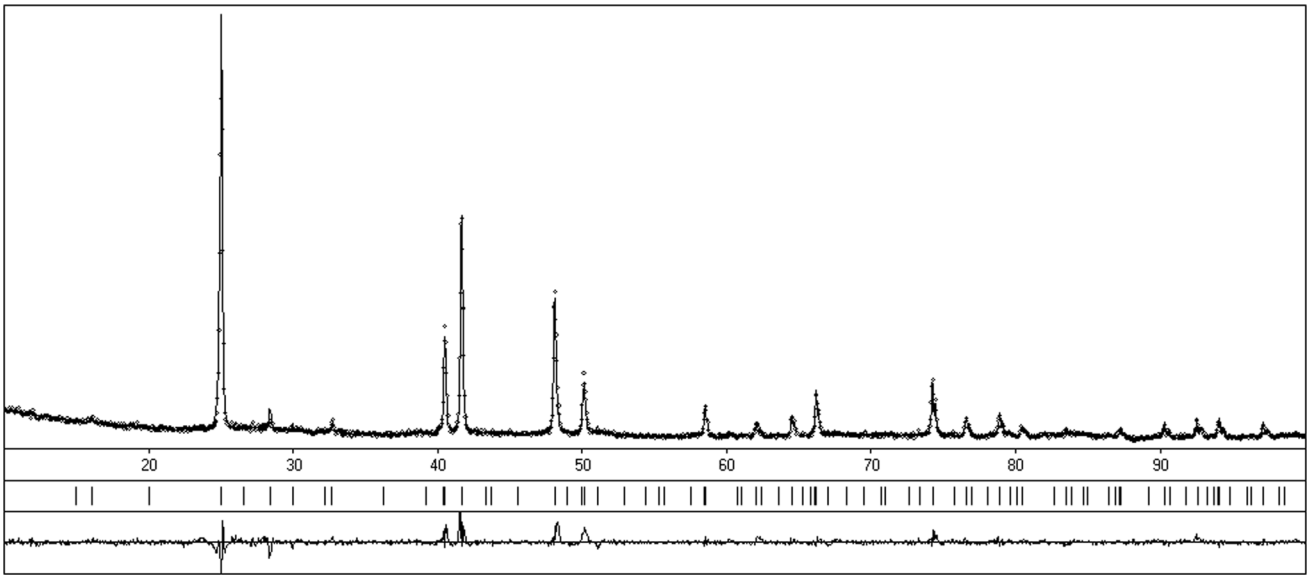

Fig. 14 Experimental (dots), calculated (solid) and difference (bottom scale) diffractogram of the $AgGa_2Te_3Br$ compound.

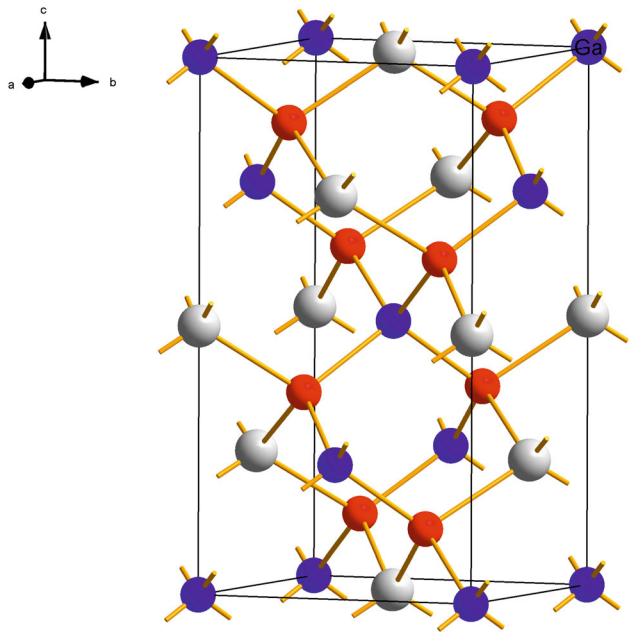

Fig. 15 The structure of the unit cell and coordination polyhedra of statistical mixtures M1, M2 and Ga atoms in the structure of $AgGa_2Te_3Br$, where blue balls-Ga1, Ga2; grey balls-M1, M2; red balls-Anion

Table 5 Coordinates of atoms in the structures of ternary and quaternary compounds

$CdGa_2Se_4$ Sp.Gr. *I*-4[17]	β-Ag_2HgI_4 Sp.Gr. *I*-4[18]	$A^IC^{III}{}_2X^{VI}{}_3Y^{VII}$ Sp.Gr. *I*-4
2*a* (0 0 0) Cd (1)	2*a* (0 0 0) Hg (1)	2*a* (0 0 0) C^{III} (0.8)
2*c* (0 ½ ¼) Ga (1)	2*c* (0 ½ ¼) Ag (1)	2*c* (0 ½ ¼) C^{III} (0.8)
2*b* (0 0 ½) Ga (1)	2*b* (0 0 ½) Ag (1)	2*b* (0 0 ½) 0.5 A^I + 0.2 C^{III}
…	…	2*d* (0 ½ ¾) 0.5 A^I + 0.2 C^{III}
8 *g* (x x z) S (1)	8 *g* (x x z) I (1)	8 *g* (x x z) 0.75 X^{VI} + 0.25 Y^{VII}

References

1. V.S. Kozak, I.A. Ivashchenko, and I.D. Olekseiuk, Phase Equilibria in the Quasi-Ternary System Cu_2Se-In_2Se_3-CuI, *Uzhhorod Univ. Sci. Bull. Chem. Ser.*, 2019, **42**, p 26-34. https://doi.org/10.24144/2414-0260.2019.2.26-34
2. K.-J. Range, H.J. Huebner, and B. Teil, Hochdrucksynthese Quaternärer Chalkogenidhalogenide AB_2X_3Y (A-Cu, Ag; B-In; X-S, Se, Te; Y-Cl, Br, I), *Anorg. Chem.*, 1983, **38**, p 155-160. https://doi.org/10.1515/znb-1983-0207
3. K.-J. Range and K. Handrick, New 13_206_37 Compounds, *Z. Naturforsch.*, 1988, **43**, p 240-242. https://doi.org/10.1515/znb-1988-0218
4. V.S. Kozak, P.V. Tyshchenko, I.D. Olekseiuk, I.A. Ivashchenko, and L.D. Gulay, Crystal Structure of $CuGa_2S(Se)_3I$ Compounds, *Odesa Univ. Sci. Bull. Chem. Ser.*, 2019, **72**, p 63-69. https://doi.org/10.18524/2304-0947.2019.4(72).185534
5. P.V. Tyshchenko, Phase Equilibria of Quasi-Triple Systems Based on the Compounds of $A^I{}_2X$, $B^{III}{}_2X_3$, R_2X_3, A^IY (A^I-Cu, Ag; B^{III}-Ga, In; R-La, Er; X-S, Se; Y-Cl, I) and Properties of Intermediate Phases and Glasses. PhD thesis. 02.00.01, Uzhgorod, 2019, 154 p. https://www.uzhnu.edu.ua/uk/infocentre/get/21024
6. I. Ivashchenko, V. Kozak, L. Gulai, and I. Olekseiuk, Crystal Structure of $AgGa_2Se_3Cl(Br)$ Compounds, *Proc. Shevchenko Sci. Soc. Chem. Sci.*, 2022, **LXX**, p 62-68. https://doi.org/10.37827/ntsh.chem.2022.70.062
7. V. Kozak, I. Ivashchenko, L. Gulay, and I. Olekseyuk, Crystal Structure of the $AgGa_2Se_3Cl$ and $AgGa_2Te_3Cl$ Compounds, *Chem. Met. Alloys*, 2020, **13**, p 45-48.
8. I.A. Ivashchenko, V.S. Kozak, L.D. Gulay, and I.D. Olekseiuk, The Crystal Structure of the Compound $AgGa_2Te_3I$, *Uzhhorod Univ. Sci. Bull. Chem. Ser.*, 2022, **47**, p 19-21. https://doi.org/10.24144/2414-0260.2022.1.19-21
9. Y. Yude, H. Boysen, and H. Schulz, Neutron Powder Investigation of CuI, *Z. Kristallogr.*, 1990, **191**, p 79-91. https://doi.org/10.1524/zkri.1990.191.1-2.79
10. L.D. Gulay, M. Daszkiewicz, O.M. Strok, and A. Pietraszko, Crystal Structure of Cu_2Se, *Chem. Met. Alloys*, 2011, **4**, p 200-205. https://doi.org/10.30970/cma4.0184
11. S. Popovic, A. Tonejc, B. Grzeta-Plencovic, B. Celustka, and R. Trojko, Revised and New Crystal Data for Indium Selenides, *J. Appl. Cryst*, 1979, **12**, p 416. https://doi.org/10.1107/S0021889879012863
12. O.F. Zmiy, I.A. Mishchenko, and I.D. Olekseyuk, Phase Equilibria in the Quasi-Ternary System Cu_2Se-$CdSe$-In_2Se_3, *J. Alloys Compd.*, 2004, **367**, p 49-57. https://doi.org/10.1016/j.jallcom.2003.08.011
13. L. Gulay, I. Ivashchenko, O. Zmiy, and I. Olekseyuk, Crystal Structure of the $CuIn_7Se_{11}$ Compound, *J. Alloys Compd.*, 2004, **384**, p 121-124. https://doi.org/10.1016/j.jallcom.2004.03.117
14. I. Ivashchenko, L. Gulay, O. Zmiy, and I. Olekseyuk, The Quasiternary System Cu_2Se-$CdSe$-In_2Se_3 and Crystal Structure of the $Cu_{0.6}Cd_{0.7}In_6Se_{10}$ Compound, *J. Alloys Compd.*, 2005, **394**, p 186-193. https://doi.org/10.1016/j.jallcom.2004.10.031
15. M.V. Moroz, M.V. Prokhorenko, S.V. Prokhorenko, M.V. Yatskov, and O.V. Reshetnyak, Thermodynamic Properties of $AgIn_2Te_3I$ and $AgIn_2Te_3Br$ Determined by EMF Method, *J. Phys. Chem.*, 2018, **92**, p 19-23. https://doi.org/10.1134/S0036024418010168
16. E. Parte, *Elements of Inorganic Structural Chemistry*, 2nd edn. Geneve, Archive ouverte UNIGE, 1996, p141
17. H. Hahn, G. Frank, W. Klingler, A.D. Strörger, and G. Strörger, Untersuchungen Über Ternäre Chalkogenide. VI. Über Ternäre Chalcogenide des Aluminiums, Galliums und Indiums mit Zink, Cadmium und Quecksilber, *Z. Anorg. Chem*, 1955, **279**, p 241-270. https://doi.org/10.1002/zaac.19552790502
18. H. Hahn, G. Frank, and W. Klingler, Zur Struktur des β-Cu_2HgJ_4 und des β-Ag_2HgJ_4, *Z. Anorg. Chem.*, 1955, **279**, p 271-280. https://doi.org/10.1002/zaac.19552790503